ChemPubSoc Europe

DOI: 10.1002/chem.201803038

CHEMISTRY
A European Journal
Communication

EPR spectroscopy | *Hot Paper*

First Demonstration of Magnetoelectric Coupling in a Polynuclear Molecular Nanomagnet: Single-Crystal EPR Studies of $[Fe_3O(O_2CPh)_6(py)_3]ClO_4$·py under Static Electric Fields

Athanassios K. Boudalis,*[a] Jérôme Robert,[a, b] and Philippe Turek[a]

Abstract: Single-crystal EPR experiments show that the highly symmetric antiferromagnetic half-integer spin triangle $[Fe_3O(O_2CPh)_6(py)_3]ClO_4$·py (**1**, py = pyridine) possesses a $S_T = 1/2$ ground state exhibiting high *g*-anisotropy due to antisymmetric exchange (Dzyaloshinskii–Moriya) interactions. EPR experiments under static electric fields parallel to the triangle's plane (i.e., perpendicular to the magnetic *z*-axis) reveal that this ground state couples to externally applied electric fields. This magnetoelectric coupling causes an increase in the intensity of the intradoublet EPR transition and does not affect its resonance position when $\mathbf{B}_0 \| \boldsymbol{z}$. The results are discussed on the basis of theoretical models correlating the spin chirality of the ground state with the magnetoelectric effect.

Electric control of magnetic materials promises to revolutionize the design of electronic devices, as it entails levels of spatial and temporal precision unattainable through magnetic fields. Sources of electric fields, such as STM tips, can easily address single molecules, or atoms, and implement switches that can turn on and off at rates of several tens of GHz. Such specifications are beyond the reach of magnetic field sources. However, this magnetoelectric control usually requires a mechanism that can couple spins to electric fields, such as the hyperfine Stark effect reported in $[Tb^{III}(pc)_2]$ ($pc^- =$ phthalocyanine anion).[1]

Interestingly, antiferromagnetic triangles of half-integer spins, or "spin triangles", are magnetic objects that lack an inversion center, and whose spin should, in principle, directly couple to external electric fields. In addition, those objects possess a rare quantum property, spin chirality, which derives from the simultaneous interplay of competing antiferromagnetic interactions and Dzyaloshinskii–Moriya interactions (DMI). Spin chirality has generated interest as it relates to diverse phenomena, such as orbital currents in Mott insulators,[2] toroidal magnetic moments in Dy^{III}_3 triangles,[3] Berry phase in spin triangles,[4] magnetic skyrmions[5] and anomalous Hall effect in chiral magnets.[6]

The scalar spin chirality in spin triangles has recently been proposed for the implementation of spin-chirality qubits, utilizing the eigenvalue of their spin chirality operator as a computational degree of freedom, instead of their spin projection. This encoding scheme, initially proposed for molecular nanomagnets (MNMs)[7,8] and then extended to clusters of atomic Cu[9] and quantum dot triads,[10] promises electric control,[7,8] practically zero decoherence from hyperfine interactions,[11] and even the possibility of quaternary logic.[12] Moreover, apart from its use in single-qubit control, the postulated magnetoelectric effect has also been proposed for long-range multiqubit coupling by the microwave electric field inside resonant cavities.[13] In the proposed schemes,[4,7,8,13,14] an electric field **E** parallel to the triangle's plane (i.e., perpendicular to the molecular magnetic *z*-axis, $\mathbf{E} \perp \boldsymbol{z}$) is proposed to couple to the spin of the ground state, allowing its electric control.

The high availability of molecular triangular magnetic systems, such as "basic" iron/chromium(III) carboxylates and copper(II) pyrazolates,[15,16] and their demonstrated stability upon surface deposition,[17] render them particularly attractive for a chemical approach to the problem of qubit implementation. EPR spectroscopy is a powerful tool towards confirming the feasibility of this approach; EPR studies under electric fields have recently been applied for the electric control of the spin states of Mn^{II} in ZnO,[18] ^{75}As and ^{31}P in Ge and Si,[19–21] while ferromagnetic resonance (FMR) has been used to study the electric control of multiferroic heterostructures.[22]

We had previously carried out[23,24] extended magnetic, X-band EPR and low-temperature synchrotron crystallographic studies on the highly-symmetric complex $[Fe_3O(O_2CPh)_6(py)_3]ClO_4$·py[25] (**1**, Figure 1, py = pyridine). Herein, we report X-band continuous wave EPR (CW-EPR) spectroscopic studies on single crystals of **1** under externally applied static electric fields and demonstrate a magnetoelectric coupling for the first time in an exchange-coupled molecule and in MNMs in general.

Single-crystal EPR spectra for **1** (Figure 2) are in line with the powder ones: they reveal a symmetric derivative spectrum at $g = 2.0$ when the molecular axis (***z***) is parallel to the Zeeman field ($\mathbf{B}_0 \| \boldsymbol{z}$), which corresponds to the $g_{0\|}$ value of the constit-

[a] Dr. A. K. Boudalis, Dr. J. Robert, Prof. P. Turek
Institut de Chimie de Strasbourg (UMR 7177, CNRS-Unistra)
Université de Strasbourg
4 rue Blaise Pascal, CS 90032
F-67081 Strasbourg (France)
E-mail: bountalis@unistra.fr

[b] Dr. J. Robert
Sorbonne Université, CNRS
Laboratoire Jean Perrin, LJP
F-75005 Paris (France)

Supporting information and the ORCID identification number(s) for the author(s) of this article can be found under:
https://doi.org/10.1002/chem.201803038.

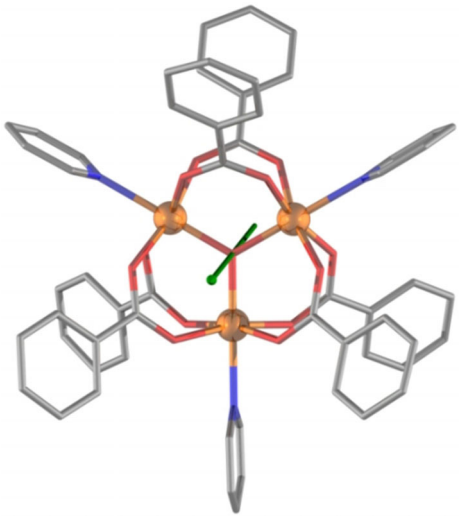

Figure 1. POV-Ray plot of the cation of **1**. The green arrow passing through the central oxide indicates the crystallographically imposed C_3 axis, running parallel to the crystallographic *c*-axis.

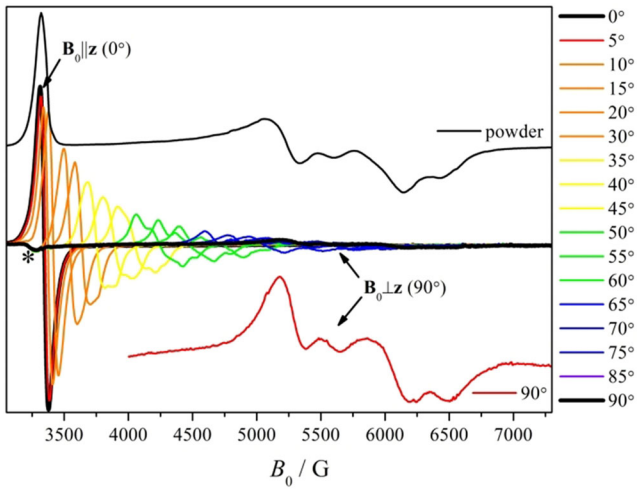

Figure 2. X-band EPR single-crystal and powder data of **1** at 4.2 K. The asterisk at ≈3300 G indicates a cavity impurity. Experimental conditions: $f = 9.31$ GHz, mod. ampl. = 10 G_{pp}. Single-crystal spectra (0–90°): Power = 2.5 mW. Single-crystal spectrum at 90° (red line): Power = 10 mW. Powder spectrum (black line): Power = 0.02 mW.

uent ions (O_h high-spin Fe^{III}). The resonance shifts to higher fields when the angle increases, accompanied by: 1) a pronounced decrease of the spectral amplitude, (≈30:1 between the 0 and 90° spectra, respectively), 2) a broadening of the lines and 3) the appearance of spectral features which we have previously attributed to atomic vibrations which lead to magnetic symmetry lowering, in conjunction with DMI.[24]

Single-crystal spectra were collected under static electric fields ($\mathbf{E}_0$) using a custom-made sample holder, suitable for brittle molecular crystals of arbitrary shapes, for use on commercial instruments (see Supporting Information). The field was applied parallel to the plane of the Fe_3 triangles as considered by Loss[7,8,11,13] and others[4,14] (i.e., $\mathbf{E}_0 \perp \boldsymbol{z}$), and rotated along with the crystal on the horizontal laboratory plane (Scheme S1). Considering an electrode distance of $r \approx 0.25$ mm, the maximum electric field for a voltage of $\Delta V = 2200$ V, was $\Delta V/r \approx 9 \times 10^6$ V m^{-1} (90 kV cm^{-1}).

For $\mathbf{B}_0 \| \boldsymbol{z}$, it was readily observed that the intensities of the spectra increased upon application of the electric field (Figure 3). For the quantification of the effect, fits with a Voigtian lineshape were carried out for each spectrum (Figure S1).

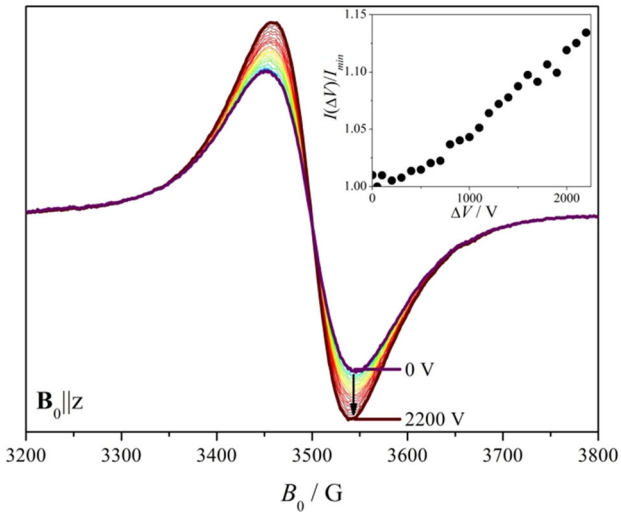

Figure 3. X-band EPR single-crystal data of **1** at $\mathbf{B}_0 \| z$ under varying electric fields. Experimental conditions: $f = 9.80$ GHz, mod. ampl. = 10 G_{pp}, power: 2 mW. The inset shows the electric field dependence of the integrated intensities of the experimental spectra ($I_{min} = 1$).

Based on those fits, the increase in amplitude was associated with an increase of intensities of the spectra (double integrals) and a decrease of their linewidth's Gaussian component, whereas the Lorentzian component remained stable; the *g*-factor was practically unaffected, within experimental error, and equal to 2.0010 ± 0.0005. The integrated intensities of the experimental data increase linearly above 500 V (Figure 3, inset).

At a 45° ($\mathbf{B}_0$,$\boldsymbol{z}$) angle the spectra exhibited a similar effect (Figure 4). Since the line shape in this case was more complicated and non-symmetric, fits were not attempted. Instead, the intensities of the experimental curves (double integrals) were extracted and compared. In comparison, between 0 and 2200 V, the 45° spectra exhibit a slightly less pronounced relative increase of their intensity (Table 1); this increase appears linear within experimental error (Figure 4, inset).

The effect was less discernible for experiments carried out at $\mathbf{B}_0 \perp \boldsymbol{z}$ (Figure 5). The main reason for this was that, due to experimental considerations (see Supporting Information), a dielectric resonator was used for studies under electric fields, whereas a high-sensitivity TE_{011} cavity was used for standard single-crystal and powder studies. The lower sensitivity of the dielectric resonator, combined with the smaller spectral amplitudes at $\mathbf{B}_0 \perp \boldsymbol{z}$ (≈3% of those at $\mathbf{B}_0 \| \boldsymbol{z}$), resulted to significantly lower S/N ratios. Double integration of the spectra indicated a +8% increase in the spectral intensity, although this figure

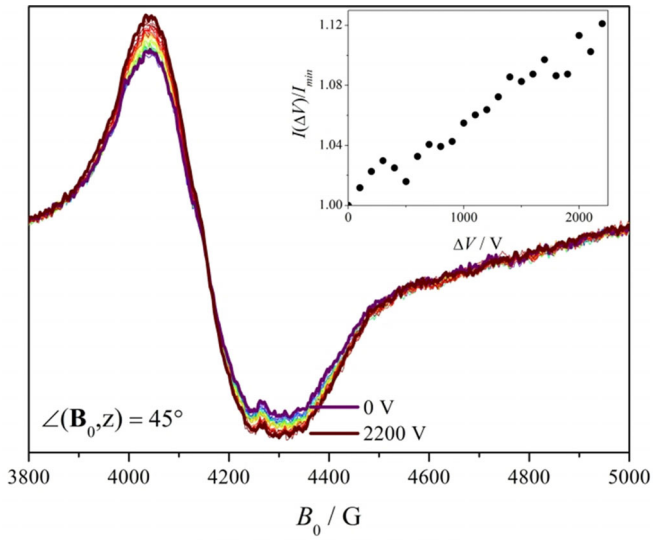

Figure 4. X-band EPR single crystal data of **1** at $\angle(\mathbf{B}_0,\mathbf{z}) = \pi/4$ under varying electric fields. Experimental conditions: $f = 9.80$ GHz, mod. ampl. = 10 G_{pp}, power: 4 mW. The inset shows the electric field dependence of the integrated intensities of the experimental spectra ($I_{min} = 1$).

Table 1. Relative changes of integrated intensities between 0 and 2200 V.

	0°	45°	90°
Intensity	+13%	+12%	+8%

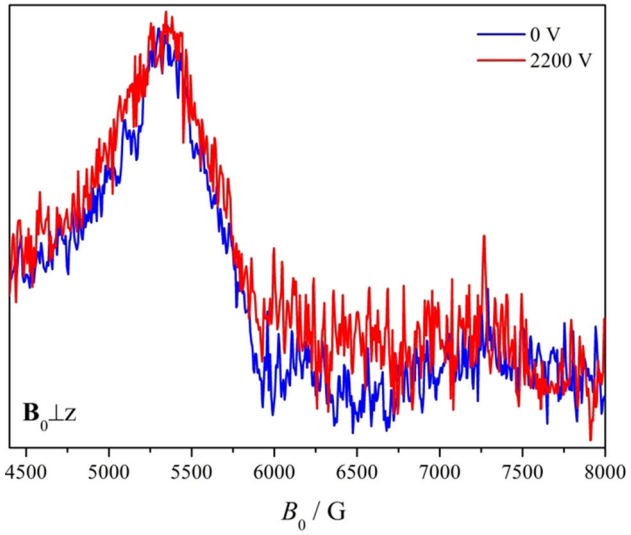

Figure 5. X-band EPR single crystal data of **1** at $\mathbf{B}_0 \perp \mathbf{z}$ inside and outside an electric field. Experimental conditions: $f = 9.80$ GHz, mod. ampl. = 15 G_{pp}, power: 6.2 mW.

should be considered with caution, given the lower sensitivity of these experiments.

The magnetic exchange within complex **1** and similar complexes are described by the general spin Hamiltonian [Eq. (1)]:

$$\hat{H} = -2\sum_{i,j=1}^{3} J_{ij}\hat{\mathbf{S}}_i \cdot \hat{\mathbf{S}}_j + 2\sum_{i,j=1}^{3} \mathbf{G}_{ij}(\hat{\mathbf{S}}_i \times \hat{\mathbf{S}}_j) \qquad (1)$$

where J_{ij} are the isotropic (Heisenberg) exchange parameters and $\mathbf{G}_{ij}$ are the pseudovectors of the antisymmetric (Dzyaloshinskii–Moriya) exchange terms and which for triangular complexes are characterized by $G_z \gg (G_x, G_y) \approx 0$ as predicted by Moriya's symmetry rules;[26] single-ion zero-field splitting does not appreciably affect the EPR spectra of these complexes, even for high single-ion D values, as we have previously shown.[24] Theoretical models have been proposed to account for the effects of static electric fields on the EPR spectra of triangles experiencing DMI. Detailed such models have been developed for triangles of $S_i = 1/2$ spins[8,27,28] and have been briefly touched upon for triangles of $S_i = 3/2$ spins,[29] but none have been explicitly worked out for $S_i = 5/2$ triangles. Loss and co-workers[8] have worked out the Stark effect on the frequencies and intensities of EPR resonances of equilateral triangles ($J_{12} = J_{23} = J_{13} = J$) for $\mathbf{E}_0 \perp \mathbf{z}$, and in two Zeeman orientations $\mathbf{B}_0 \parallel \mathbf{z}$ and $\mathbf{B}_0 \perp \mathbf{z}$. Belinsky[27,28] has worked out the influence of an $\mathbf{E}_0 \perp \mathbf{z}$ field on equilateral, isosceles ($J_{12} = J_{23} = J \neq J_{23} = J'$) and scalene ($J_{12} \neq J_{23} \neq J_{13} \neq J_{12}$) triangles, and has given a detailed description of the relations between vector chirality $\hat{\mathbf{K}}$, the scalar chirality $\hat{\mathbf{C}}$, the spin configurations and magnetizations in all those cases. In particular, for an isosceles triangle in $\mathbf{B}_0 \parallel \mathbf{z}$, the four low-lying states are divided into two doublets, with the ground doublet being characterized by an intermediate spin $S_{12} = 0$ (for $|J| < |J'|$) or $S_{12} = 1$ (for $|J| > |J'|$), and by a right-handed vector chirality ($\kappa = +1$) for $G_z < 0$ or left-handed chirality ($\kappa = -1$) for $G_z > 0$. Each Zeeman sublevel is characterized by scalar chirality $\chi = 2\kappa M_s = \pm 1$ (Figure S2). Therefore, the classical EPR intradoublet transition conserves the vector chirality and the intermediate spin, and reverses the scalar chirality ($\Delta\chi = \pm 2$) and spin projection ($\Delta M_s = \pm 1$). For $G_z = 0$ the system is achiral ($\chi = \kappa = 0$), while for an equilateral system ($J = J'$) the states possess no S_{12} character.[28]

Focusing on the ground $|\chi, M_s\rangle$ doublet of an equilateral triangle, Loss and co-workers[8] have calculated the effect of an electric field $\mathbf{E}_0 \perp \mathbf{z}$ on the intensity of the intradoublet $|-1/2, +1\rangle \leftrightarrow |+1/2, -1\rangle$ EPR transition as proportional to [Eq. (2)]:

$$|\langle -1/2,\ +1|S_x|+1/2,\ -1\rangle|^2 = |-\varepsilon^2/D^{+1}D^{-1}|^2 \qquad (2)$$

where $\varepsilon = d \cdot E$ and $D^{\chi} = \{\varepsilon^2 + [\Delta + \chi(\varepsilon^2 + \Delta^2)^{1/2}]^2\}^{1/2}$. In these expressions d is the dipolar coupling constant and Δ is the energy separation between the two doublets, which is considered to be solely due to DMI and not to any magnetic asymmetry. Equation (2) implies zero transition probability at $\mathbf{E}_{0\perp} = 0$, which indeed is the case for an equilateral triangle;[30,31] in that sense, the role of a $\mathbf{E}_0 \perp \mathbf{z}$ field is to break the equilateral symmetry by modifying the J_{ij} parameters. For lower magnetic symmetries ($\Delta J = J - J' \neq 0$) this is an allowed EPR transition even for $\mathbf{E}_{0\perp} = 0$, and Belinsky shows[28] that the increase of ΔJ would increase its intensity. Ab initio calculations by Islam et al.[14] on an equilateral Cu^{II}_3 polyoxovanadate have indicated that a field $\mathbf{E}_0 \perp \mathbf{z}$ of ca. $10^7\ V\,m^{-1}$, that is, comparable to ours, would increase ΔJ by ca. $2 \times 10^{-3}\ cm^{-1}$; this, in turn, would increase the intradoublet transition intensity, according to Belinsky. However, Belinsky provides no analytical expressions for the EPR transition probabilities as a function of the applied

electric field in the general case of an asymmetric triangle. As for the resonance position, both Loss[8] and Belinksy[28] predict that the intradoublet $\mathbf{B}_0 \| \boldsymbol{z}$ transition will not shift in energy under the influence of an electric field $\mathbf{E}_0 \perp \boldsymbol{z}$.

From a qualitative point of view, our observations confirm the theoretical predictions of Belinsky and of Loss. There is indeed a magnetoelectric coupling as predicted from symmetry arguments. Also as predicted, the intradoublet transition increases in intensity with the application of an electric field $\mathbf{E}_0 \perp \boldsymbol{z}$, and its resonance position remains unshifted when $\mathbf{B}_0 \| \boldsymbol{z}$. This increase in intensity is in line with an increase in magnetic deformation, though other mechanisms may also be operative. It should also be noted that, theoretically, such a decrease in magnetic symmetry would also be reflected on the position of the transition at $\mathbf{B}_0 \perp \boldsymbol{z}$, as the effective $g_\perp$ is determined by the relation between ΔJ and G_z.[30,31] However, the lower sensitivity at that orientation does not allow us to make that determination. Finally, our observations regarding the line shapes upon application of electric fields, that is, narrowing and increase in peak-to-peak amplitude, are not predicted by either model at the considered level of precision.

The EPR signal response to an external electric field should, in principle, allow the direct determination of the electric dipole coupling constant, *d*, for our complex. However, quantitative analyses are not currently possible, as the case of a $S_i = 5/2$ triangle has not been worked out.

In addition, the electric field effect would need to be explicitly considered in conjunction with the dielectric constant of the crystal. While the above-mentioned models refer to effective electric fields experienced by isolated molecules, molecules in real crystals will tend to experience a significantly different electric field than calculated by $\Delta V/r$. We therefore need to consider both the depolarizing field that will reduce the macroscopic field within the crystal, as well as the local Lorentz field experienced by the molecular sites in the crystal. Since, however, the material's dielectric constant cannot be assumed, it must be determined for the particular experimental conditions. Indeed, it is known that the dielectric constant of a given material depends on the temperature and the electric field frequency, and it was recently shown that in the case of two molecular ferromagnets, it can also heavily depend on the applied magnetic field.[32] Therefore, to safely quantify the applied field on the molecular sites, precise such determinations are necessary for **1**.

The reported magnetoelectric coupling is a critical prerequisite for the electric control of spin qubits. In the present context it affords preliminary confirmation to the prediction that oscillating electric fields can induce scalar chirality inversions in spin-chiral systems, thus encoding spin qubits with long decoherence times. In the broader context of spin-electric coupling in MNMs, it demonstrates that direct magnetoelectric coupling is possible based on symmetry considerations alone, without the need of additional mechanisms, such as hyperfine interactions, thus broadening the scope and applicability of the effect.

In conclusion, we have confirmed the magnetoelectric coupling predicted for spin triangles under electric fields. This is, actually, the first such experimental confirmation in molecular exchange-coupled polynuclear systems, for the purposes of which we developed a custom sample holder. We are currently working toward increasing the maximum electric field, to reach beyond the linear region of the signal increase, and toward experiments at other orientations of the electric field with respect to the molecular *z*-axis (e.g., $\mathbf{E}_0 \| \boldsymbol{z}$). We are also working towards developing theoretical models for the treatment of $S_i = 5/2$ triangles and determining the dielectric constant of **1** to accurately determine the electric fields at the molecule sites inside the crystal. At the same time, we are planning similar studies on Cu^{II}_3 and Cr^{III}_3 triangles, for which the theoretical framework is better developed.

Acknowledgements

We thank Prof. Daniel Loss for helpful discussions on theoretical aspects and experimental design, Dr. Yiannis Sanakis for discussions on the EPR spectroscopy of spin triangles,the CNRS for the temporary assignment of J.R. at the Institut de Chimie de Strasbourg for the duration of this work, and the national French EPR network RENARD (IR-RPE CNRS 3443) for support. This project has received funding from the European Union's Horizon 2020 research and innovation programme under the Marie Sklodowska-Curie grant agreement No. 746060 (project "CHIRALQUBIT").

Conflict of interest

The authors declare no conflict of interest.

Keywords: EPR spectroscopy · molecular nanomagnets · spin chirality · spin triangles · spin-electric coupling

[1] S. Thiele, F. Balestro, R. Ballou, S. Klyatskaya, M. Ruben, W. Wernsdorfer, *Science* **2014**, *344*, 1135 – 1138.
[2] L. N. Bulaevskii, C. D. Batista, M. V. Mostovoy, D. I. Khomskii, *Phys. Rev. B* **2008**, *78*, 024402.
[3] D. I. Plokhov, A. K. Zvezdin, A. I. Popov, *Phys. Rev. B* **2011**, *83*, 184415.
[4] V. A. Mousolou, C. M. Canali, E. Sjöqvist, *Phys. Rev. B* **2016**, *94*, 235423.
[5] J. Matsuno, N. Ogawa, K. Yasuda, F. Kagawa, W. Koshibae, N. Nagaosa, Y. Tokura, M. Kawasaki, *Sci. Adv.* **2016**, *2*, e1600304.
[6] H. Ishizuka, N. Nagaosa, *Sci. Adv.* **2018**, *4*, eaap9962.
[7] M. Trif, F. Troiani, D. Stepanenko, D. Loss, *Phys. Rev. Lett.* **2008**, *101*, 217201.
[8] M. Trif, F. Troiani, D. Stepanenko, D. Loss, *Phys. Rev. B* **2010**, *82*, 045429.
[9] B. Georgeot, F. Mila, *Phys. Rev. Lett.* **2010**, *104*, 200502.
[10] C.-Y. Hsieh, P. Hawrylak, *Phys. Rev. B* **2010**, *82*, 205311.
[11] F. Troiani, D. Stepanenko, D. Loss, *Phys. Rev. B* **2012**, *86*, 161409.
[12] D. I. Khomskii, *J. Phys. Condens. Matter* **2010**, *22*, 164209.
[13] D. Stepanenko, M. Trif, O. Tsyplyatyev, D. Loss, *Semicond. Sci. Technol.* **2016**, *31*, 094003.
[14] M. F. Islam, J. F. Nossa, C. M. Canali, M. Pederson, *Phys. Rev. B* **2010**, *82*, 155446.
[15] P. A. Angaridis, P. Baran, R. Boča, F. Cervantes-Lee, W. Haase, G. Mezei, R. G. Raptis, R. Werner, *Inorg. Chem.* **2002**, *41*, 2219 – 2228.
[16] A. K. Boudalis, G. Rogez, B. Heinrich, R. G. Raptis, P. Turek, *Dalton Trans.* **2017**, *46*, 12263 – 12273.
[17] V. Corradini, C. Cervetti, A. Ghirri, R. Biagi, U. del Pennino, G. A. Timco, R. E. P. Winpenny, M. Affronte, *New J. Chem.* **2011**, *35*, 1683.

[18] R. E. George, J. P. Edwards, A. Ardavan, *Phys. Rev. Lett.* **2013**, *110*, 027601.
[19] A. J. Sigillito, A. M. Tyryshkin, S. A. Lyon, *Phys. Rev. Lett.* **2015**, *114*, 217601.
[20] A. J. Sigillito, A. M. Tyryshkin, J. W. Beeman, E. E. Haller, K. M. Itoh, S. A. Lyon, *Phys. Rev. B* **2016**, *94*, 125204.
[21] A. J. Sigillito, A. M. Tyryshkin, T. Schenkel, A. A. Houck, S. A. Lyon, *Nat. Nanotechnol.* **2017**, *12*, 958 – 962.
[22] J. Lou, M. Liu, D. Reed, Y. Ren, N. X. Sun, *Adv. Mater.* **2009**, *21*, 4711 – 4715.
[23] A. N. Georgopoulou, Y. Sanakis, A. K. Boudalis, *Dalton Trans.* **2011**, *40*, 6371.
[24] A. N. Georgopoulou, I. Margiolaki, V. Psycharis, A. K. Boudalis, *Inorg. Chem.* **2017**, *56*, 762 – 772.
[25] F. E. Sowrey, C. Tilford, S. Wocadlo, C. E. Anson, A. K. Powell, S. M. Bennington, W. Montfrooij, U. A. Jayasooriya, R. D. Cannon, *J. Chem. Soc. Dalton Trans.* **2001**, 862 – 866.
[26] T. Moriya, *Phys. Rev.* **1960**, *120*, 91 – 98.
[27] M. I. Belinsky, *Chem. Phys.* **2014**, *435*, 62 – 94.
[28] M. I. Belinsky, *Chem. Phys.* **2014**, *435*, 95 – 125.
[29] M. Trif, *Spin-Electric Coupling in Quantum Dots and Molecular Magnets*, Ph.D. Thesis, University of Basel, **2011**.
[30] Yu. V. Rakitin, Y. V. Yablokov, V. V. Zelentsov, *J. Magn. Reson.(1969)* **1981**, *43*, 288 – 301.
[31] B. Tsukerblat, M. Belinskii, V. Fainzil'berg, *Soviet Sci. Rev. B* **1987**, 337 – 482.
[32] L. Yang, J. Li, T.-C. Pu, M. Kong, J. Zhang, Y. Song, *RSC Adv.* **2017**, *7*, 47913 – 47919.

Manuscript received: June 14, 2018
Accepted manuscript online: August 22, 2018
Version of record online: ■■ ▮▮, 0000

COMMUNICATION

EPR spectroscopy

A. K. Boudalis, J. Robert, P. Turek*

■■ – ■■

First Demonstration of Magnetoelectric Coupling in a Polynuclear Molecular Nanomagnet: Single-Crystal EPR Studies of $[Fe_3O(O_2CPh)_6(py)_3]ClO_4$·py under Static Electric Fields

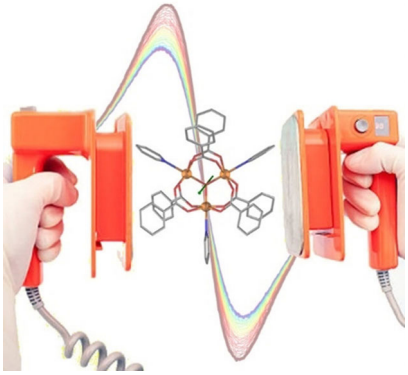

Clear! An electric field applied on the antiferromagnetic spin-chiral complex $[Fe_3O(O_2CPh)_6(py)_3]ClO_4$·py couples to the spin of its ground state and modifies its Electron Paramagnetic Resonance (EPR) spectrum. This magnetoelectric coupling can provide electric control of the spin states of Molecular Nanomagnets.